Study of electronic and vibronic contributions to cooperative enhancement of two-photon absorption in multibranched structures

Jianqiang Xue,[ab] Yuxia Zhao,*[a] Jie Wu,[a] Feipeng Wu*[a] and Xiangyun Fang[a]

Received (in Montpellier, France) 12th August 2008, Accepted 27th October 2008
First published as an Advance Article on the web 11th December 2008
DOI: 10.1039/b814013h

A series of multibranched benzylidene cyclopentanone dyes with non-conjugated central moiety were synthesized. Their one- and two-photon photophysical properties were systematically studied in comparison with corresponding triphenylamine derivatives. Electronic coupling and vibronic coupling contributions to cooperative enhancement of two-photon absorption in multibranched structure were revealed. The results showed that the crucial contribution for this enhancement was from electronic coupling effect among branches. In addition, no contribution of vibronic coupling was observed. Furthermore, multibranched effect on photosensitizing efficiency of these compounds was investigated by one-photon polymerization and the result indicated the electronic coupling effect was also beneficial to their photosensitizing efficiency.

1. Introduction

Though two-photon absorption (TPA) was theoretically predicted in 1931 and experimentally observed in 1961,[1,2] this phenomenon did not receive much attention and development until a variety of its applications were exploited in the 1990s, including two-photon-excited fluorescence microscopy,[3] high-density optical data storage,[4] three-dimensional micro-fabrication,[5] optical limiting,[6] and photodynamic therapy.[7] For these applications, compounds with large TPA cross-sections are intensely required. In last decade, many design strategies were reported to disclose the relationship of molecular structures and their TPA properties.[8–12] Among them, the discovery of cooperative enhancement of TPA in multibranched structures by Prasad *et al.* was a very important and representative work.[10] Hereafter, large numbers of multibranched or dendritic structures were investigated for developing compounds with strong TPA capability.[13–22] The cooperative enhancement was confirmed in most of them. However, their enhanced extents were quite different.[13,20,21] Furthermore, some experimental results were conflicting to this enhancement.[19,22] Evidently more efforts were needed to establish the mechanism of such a cooperative enhancement. Prasad *et al.* attributed this phenomenon partly to the electronic coupling among branches.[10] However, Luo *et al.* revealed that the enhancement was mainly caused by the vibronic coupling due to the increase of states density.[23] Both of their opinions were deduced by theoretical calculations and lacked direct support from experimental data.

Triphenylamine derivatives are the most favored compounds for researchers because they are easy to be modified and usually exhibit significant enhancement of TPA cross-sections. Till now, most reported multibranched or dendritic structures are triphenylamine derivatives.[10,15–18] Our group have also reported two series of such compounds and certain observed cooperative enhancement.[24,25] Due to the cross-conjugation effect of the central triphenylamine moiety, both electronic coupling and vibronic coupling contributions are involved in these compounds, so it is difficult to evaluate which one is the primary contributor. In this work, based on reported compounds **1–3**,[24] we design a series of novel multibranched benzylidene cyclopentanone dyes **T1–T3** (shown in Fig. 1) with a non-conjugated central moiety. Because of the absence of electronic coupling effects in these novel compounds, it is possible to study the vibronic coupling contribution solely. In addition, benzylidene cyclopentanone dyes are highly efficient photosensitizers in common photopolymerization.[26,27] In our previous work, it was shown that multibranched compounds **2** and **3** not only had larger TPA ability but also presented higher sensitizing efficiency compared to one-branched compound **1**.[24] In this work, we study the photosensitizing efficiencies of these two series of compounds and the effect of electronic coupling on the photochemical properties of multibranched compounds is revealed.

2. Experimental

2.1 Materials

The synthesis of compounds **1–3** has been described elsewhere.[24] 2-[4-(Dimethylamino)benzylidene]cyclopentanone (DMA) was synthesized according to the literature.[28] 4-Dimethyldiphenyliodonium hexafluorophosphate (Omnicat 820) was from TH-UNIS Insight Co. Ltd. 2-Phenoxyethyl acrylate (SR339), pentaerythritol triacrylate (SR444) and epoxy acrylate (CN124A80) were from Sartomer Co. Ltd., and used as received. Triethanolamine, *N*-methyldiethanolamine, dichlorosulfide, *p*-hydroxylbenzaldehyde, *p*-methoxylbenzaldehyde, fluorescein and other A.R. grade solvents were all

[a] *Key Laboratory of Photochemical Conversion and Optoelectronic Materials, Technical Institute of Physics and Chemistry, Chinese Academy of Sciences, Beijing, 100190, PR. China. E-mail: yuxia.zhao@mail.ipc.ac.cn. E-mail: fpwu@mail.ipc.ac.cn; Fax: +86 10 82543491; Tel: +86 10 82543571*
[b] *Graduate University of Chinese Academy of Sciences, Beijing, 100049, PR. China*

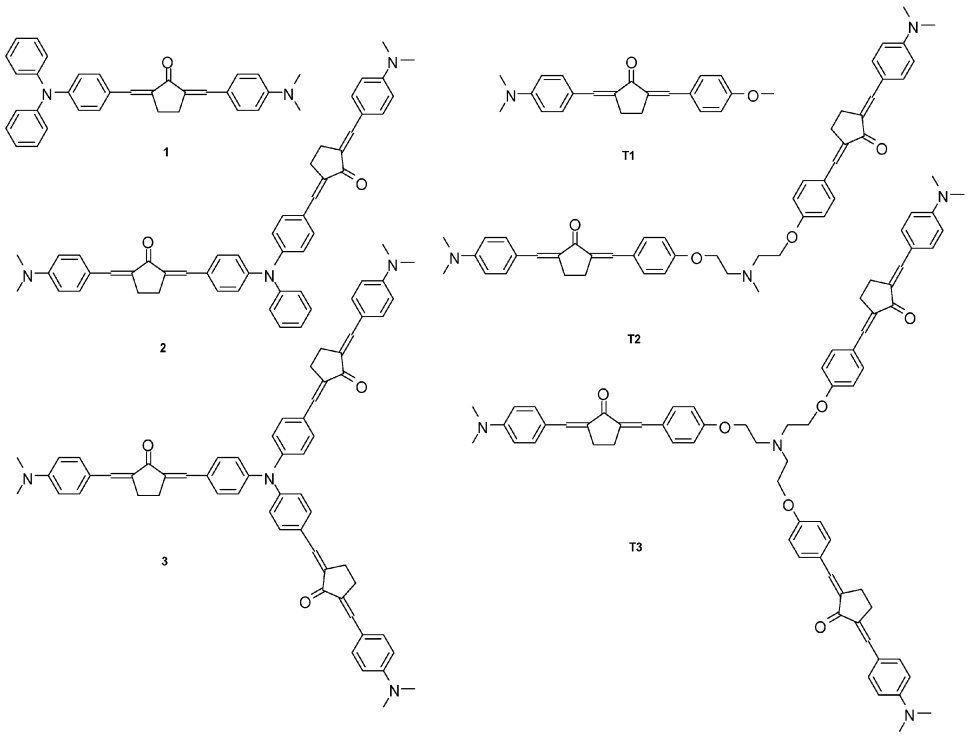

Fig. 1 Chemical structures of **T1–T3** and **1–3**.

from Beijing Chemical Reagent Company, and used after purification by common methods.

The synthetic routes to compounds **T1–T3** are shown in Scheme 1.

S3. Triethanolamine was neutralized by concentrated hydrochloric acid to yield triethanolamine hydrochloride following the literature procedure.[29] After drying in vacuum, the salt (23.2 g, 0.125 mol) was added into the solution of $SOCl_2$ (0.5 mol) in benzene (37.5 ml) in four portions. The mixture was stirred at room temperature for 1 h and then at 55 °C for 3 h. The volatile composition was distilled off and the residue was recrystallized from acetone to obtain tris(2-chloroethyl)amine hydrochloride with a total yield of 67%, mp 124 °C [lit.,[30] 130–131 °C]. **S3** was synthesized from tris(2-chloroethyl)amine hydrochloride and *p*-hydroxylbenzaldehyde according to the literature[31] and characterized by ^{1}H NMR (400 MHz, $CDCl_3$, TMS) δ: 3.21 (t, *J* 5.1 Hz, 6 H), 4.18 (t, *J* 5.1 Hz, 6 H), 6.96 (d, *J* 8.4 Hz, 6 H), 7.81 (d, *J* 8.5 Hz, 6 H), 9.88 (s, 3 H), HR-MS (ESI): Anal. Calc. for $C_{27}H_{28}NO_6$ [M + H]: 462.19111. Found: 462.19104, mp 92 °C [lit.,[31] 80–82 °C].

S2. Bis(2-chloroethyl)methylamine hydrochloride was synthesized from *N*-methyldiethanolamine and $SOCl_2$ following the similar procedure described by Wilson,[32] mp 108–110 °C. **S2** was prepared following the similar procedure of **S3** and characterized by ^{1}H NMR (400 MHz, $CDCl_3$, TMS) δ: 2.47 (s, 3 H), 2.97 (t, *J* 5.6 Hz, 4 H), 4.16 (t, *J* 5.6 Hz, 4 H), 6.97 (d, *J* 8.7 Hz, 4 H), 7.79 (d, *J* 8.7 Hz, 4 H), 9.85 (s, 2 H); mp 60–61 °C.

T1. *p*-Methoxybenzaldehyde (3 mmol, 0.44 g) and DMA (3 mmol, 0.645 g) were dissolved in ethanol (15 ml) together with NaOH (0.06 g). The mixture was heated to reflux for 6 h under stirring and protected by dry N_2. After cooling to room

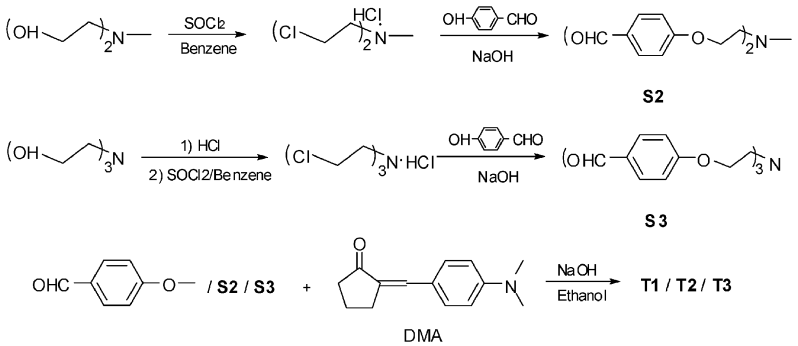

Scheme 1 Synthetic routes to **T1–T3**.

temperature, the orange precipitate was collected and washed with ethanol. The crude product was purified by column chromatography on a silica gel column using dichloromethane and ethanol as the eluent ($V_{CH_2Cl_2}$: V_{EtOH} = 100 : 1), yield 50%, and characterized by ^{1}H NMR (400 MHz, $CDCl_3$, TMS) δ: 3.05 (s, 6 H), 3.08 (s, 4 H), 3.86 (s, 3 H), 6.78 (d, J 7.9 Hz, 2 H), 6.96 (d, J 8.8 Hz, 2 H), 7.55 (m, 6 H). HR-MS (ESI): Anal. Calc. for $C_{22}H_{24}NO_2$ [M + H]: 334.18016. Found: 334.18014.

T2 and T3. Following the similar procedure of **T1**, **S2** and **S3** reacted with DMA to obtain **T2** and **T3**, respectively. The crude products were purified by column chromatography on silica gel column using dichloromethane and ethanol as the eluent ($V_{CH_2Cl_2}$: V_{EtOH} = 100 : 2), and yields were 47 and 30%, respectively. The target compounds were characterized by ^{1}H NMR and HR-MS. **T2** (400 MHz, [D_5] pyridine, TMS) δ: 2.44 (s, 3 H), 2.83 (s, 20 H), 2.96 (t, J 5.8 Hz, 4 H), 4.21 (t, J 5.7 Hz, 4 H), 6.76 (d, J 8.8 Hz, 4 H), 7.14 (d, J 8.5 Hz, 4 H), 7.64 (m, 12 H). HR-MS (ESI): Anal. Calc. for $C_{47}H_{52}N_3O_4$ [M + H]: 722.39523. Found: 722.39508. **T3** ^{1}H NMR (400 MHz, $CDCl_3$, TMS) δ: 3.03 (s, 30 H), 3.18 (d, J 5.6 Hz, 6 H), 4.14 (d, J 5.6 Hz, 6 H), 6.70 (d, J 8.6 Hz, 6 H), 6.91 (d, J 8.0 Hz 6 H), 7.51 (m, 18 H). HR-MS (FAB): Anal. Calc. for $C_{69}H_{73}N_4O_6$ [M + H]: 1053.55243. Found: 1053.55349.

2.2 Methods

UV-Vis absorption spectra were measured on a Jasco V-530 spectrophotometer. One-photon fluorescence spectra were performed on a Hitachi F-4500 fluorescence spectrophotometer. FT-IR spectra were monitored on a Varian Excalibur HE 3100 spectrophotometer. ^{1}H NMR spectra were obtained on a Bruker DPX400 spectrometer. Mass spectra were carried out on Bruker Apex_IV_FT.

Solvatochromism effects of compounds were explored in a series of mixed solvents of acetonitrile–toluene with a concentration of 10^{-5} M. The polarity of solvent was represented by the solvent polarity functions $f(\varepsilon, n)$ and $g(n)$, which was calculated from solvent's refractive index (n) and dielectric constant (ε) by eqn (1) and (2). Based on quantum mechanical perturbation theory, equations $\tilde{\nu}_a - \tilde{\nu}_f = m_1 f(\varepsilon,n)$ + const. and $\tilde{\nu}_a + \tilde{\nu}_f = -m_2\,[f(\varepsilon,n) + 2g(n)]$ + const, were obtained. Here, $\tilde{\nu}$ is the wavenumber, subscript a refers to absorption and subscript f refers to fluorescence, the parameters m_1 and m_2 can be determined by fitting $\tilde{\nu}_a - \tilde{\nu}_f$ *vs.* $f(\varepsilon,n)$ and $\tilde{\nu}_a + \tilde{\nu}_f$ *vs.* $f(\varepsilon,n) + 2g(n)$, respectively.[33–35]

$$f(\varepsilon, n) = \frac{2n^2+1}{n^2+2}\left[\frac{\varepsilon-1}{\varepsilon+2} - \frac{n^2-1}{n^2+2}\right] \quad (1)$$

$$g(n) = \frac{3}{2}\left[\frac{n^4-1}{(n^2+2)^2}\right] \quad (2)$$

Supposing the ground and excited states are parallel, their dipole moments could be expressed by eqn (3) and (4). Here, μ_g is the ground state dipole moment, μ_e is the excited state dipole moment, the Onsager radius of solute (a) is calculated using Gaussian 03 package, the calculation method was RHF in the 6-31G* basis.

$$\mu_g = \frac{m_2 - m_1}{2}\left[\frac{hca^3}{2m_1}\right]^{1/2} \quad (3)$$

$$\mu_e = \frac{m_2 + m_1}{2}\left[\frac{hca^3}{2m_1}\right]^{1/2} \quad (4)$$

The fluorescence quantum yields of **T1–T3** in chloroform were determined by using fluorescein (in 0.1 M NaOH, water) as a standard and refractive index correction was performed.[36] Fluorescence lifetimes were measured using time-correlated single-photon counting technique with a gated hydrogen discharge lamp as excitation source (Edinburgh nF9000).

TPA cross-section (δ) of compounds in chloroform (2×10^{-4} M) were determined using the two-photon-excited fluorescence (TPEF) technique with femtosecond laser pulses following the experimental protocol described in detail by Xu and Webb.[37] The excitation light sources were a mode-locked Tsunami Ti:sapphire laser (720–880 nm, 80 MHz, <130 fs) and OPA-800CF plus SHG (840–1100 nm, 1000 Hz, <200 fs). An aqueous solution of fluorescein (10^{-4} M) with 0.1 M NaOH was used as reference. To avoid any contribution from other photophysical/photochemical processes, the intensity of input pulses were adjusted to a proper regime to ensure a quadratic dependence of the fluorescence intensity *vs.* excitation pulse energy. δ was calculated by the following equation:

$$\delta = \frac{S_s \Phi_r \varphi_r c_r}{S_r \Phi_s \varphi_s c_s}\delta_r$$

Here, subscripts r and s stand for the reference and sample, respectively; S is the integral area of the two-photon-excited fluorescence; Φ is the quantum yield; φ is the overall fluorescence collection efficiency of the experimental apparatus; and c is the number density of the molecules in solution.

The experimental conditions of one-photon photopolymerization were the same as we reported before[24] except the irradiation source was changed to a miniature 473 nm laser. Its intensity of irradiation was 22 mW cm^{-2}. The co-initiator was Omnicat 820 (4×10^{-2} mol kg^{-1}). Compounds **1–3** and **T1–T3** (1×10^{-4} mol kg^{-1}) were used as sensitizers.

3. Results and discussion

3.1 Photophysical properties

The absorption and emission spectra of the compounds in chloroform are shown in Fig. 2 and their corresponding photophysical properties are listed in Table 1. It is interesting to notice that the absorption and emission spectra of **T1–T3** overlapped very well. The ratio of their molar absorption coefficients (ε_{max}) and maximum absorption peak areas (S) are 1 : 1.98 : 2.84 and 1 : 2.04 : 2.90, respectively, perfectly proportional to 1 : 2 : 3. This indicates the absence of any coupling effect among branches in **T2** and **T3** and increasing the branch number simply increases the number density of chromophores. The decreased fluorescence quantum yield (Φ) from **T1** to **T3** should be due to the concentration quench

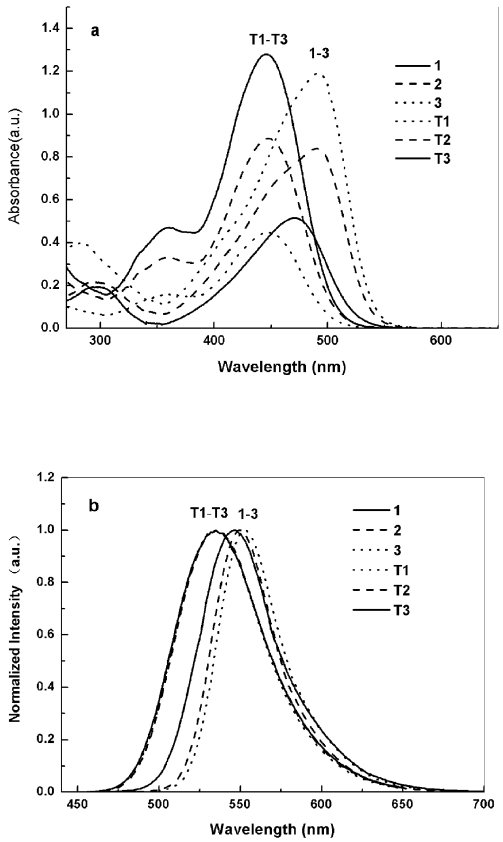

Fig. 2 Absorption (a, [dye] = 1×10^{-5} M) and normalized emission spectra (b, [dye] = 1×10^{-6} M) of compounds **1–3** and **T1–T3** in chloroform.

effect. Contrarily, both absorption and emission peaks of **1–3** show a significant red-shift with increasing number of branches. Moreover, the ratio of the ε_{max} and S of **1–3** are 1 : 1.65 : 2.33 and 1 : 1.87 : 2.57, respectively. The discrepancy of these values means the peak shapes of **1–3** are quite different, which can be clearly seen in Fig. 2. Obviously, this is due to an electronic coupling effect among branches in **2** and **3**, resulting in charge redistribution and extended delocalization. The increased fluorescence quantum yield and fluorescence lifetime from **1** to **3** also support this explanation. The extended conjugation of **2**, **3** can stabilize their excited states and their large rigid structures reduce the probability of non-irradiative deactivation.

3.2 Solvatochromism

Absorption and emission maxima of compounds in mixed solvents of toluene–acetonitrile with different polarity are listed in Table 2. It shows that the absorption peaks of all compounds present no significant shift while their emission spectra have large red-shift following the increase of solvent polarity, which implies that the polarities of their excited states are somewhat larger than those of their ground states. Fig. 3 shows the spectral shifts (in cm^{-1}) $\tilde{\nu}_a - \tilde{\nu}_f$ and $\tilde{\nu}_a + \tilde{\nu}_f$ of all compounds *versus* polarity functions $f(\varepsilon,n)$ and $f(\varepsilon,n) + 2g(n)$. Excellent linear relationships are found for all compounds, which suggests that it is feasible using this model to calculate their μ_g and μ_e values. From exactly the same plots of compounds **T1–T3**, the absence of interaction among branches is confirmed and so the same Onsager radii of them are assumed. Certain differences of $\tilde{\nu}_a - \tilde{\nu}_f$ and $\tilde{\nu}_a + \tilde{\nu}_f$ for **1–3** are observed. This suggests that electronic coupling has an influence on their charge localizations and their Onsager radii should be considered separately. Based on eqn (1)–(4), we calculate μ_g and μ_e of all compounds (listed in Table 3). The results show that the changes in the dipole moments ($\Delta\mu = \mu_e - \mu_g$) of **T1–T3** are almost the same while an increase from **1** to **3** is obtained. It further proves that no coupling effect occurs among **T1–T3** while there is increased excited state charge transfer with increased branch number from **1** to **3**. In addition, the $\Delta\mu$ of **1–3** are significantly larger than those of **T1–T3**, which should due to the stronger electron-donating capability of triphenylamine of **1–3** compared to the alkoxyl groups of **T1–T3**.

3.3 Two-photon absorption

The two-photon fluorescence excitation spectra of **T1–T3** were measured over a broad range of 710–1000 nm and are shown in Fig. 4. The small discrepancy of data from different excited sources within their overlapped area may be due to different peak power, pulse width and frequency between Tsunami and OPA plus SHG excitation sources. Thus, within measurement error, this discrepancy is acceptable and these data can be considered have good consistency with each other. Two TPA peaks are observed at the range 840–1000 nm and below 740 nm for **T1–T3**. Taking **T1** for example, when putting its one-photon absorption and TPA bands together, it shows clearly that these two bands correspond to S_0–S_1 and S_0–S_2 transitions, respectively (Fig. 5(a)). For **1–3**, the TPA peaks

Table 1 One- and two-photon optical properties of compounds **1–3**[a] and **T1–T3** in chloroform

Compound	λ_{max}^{a}[b]/nm	$10^{-5}\varepsilon_{max}$[c]/M^{-1} cm^{-1}	S[d]	λ_{max}^{fl}[b]/nm	$10^{-3}\Delta\nu$[e]/cm^{-1}	Φ[f]	δ_{max} (GM)[g]	λ_{max}^{TPA}[h]/nm	τ_t[i]/ns
T1	445.0	0.45	44.73	535.0	3.68	0.22	86	930	0.88
T2	445.5	0.89	91.26	536.0	3.71	0.15	179	940	1.01
T3	445.0	1.28	129.72	535.4	3.74	0.16	185	940	0.86
1	470.5	0.51	45.32	546.4	2.95	0.11	781	790	0.84
2	490.5	0.84	84.86	550.0	2.21	0.15	2475	790	1.05
3	492	1.19	116.58	552.6	2.23	0.16	3299	790	1.14

[a] The data of **1–3** are from the literature[24] except for τ_t. [b] λ_{max}^{a} and λ_{max}^{fl} are absorption and emission maxima, respectively. [c] ε_{max} is the corresponding molar absorption coefficient. [d] S is the peak area of main absorption band, integrated within 300–550 nm for **T1–T3** and within 350–600 nm for **1–3**. [e] $\Delta\nu$ is the Stokes shift. [f] Φ is the fluorescence quantum yield. [g] δ_{max} is the maximum δ within measured range. [h] λ_{max}^{TPA} is the corresponding wavelength of δ_{max}. [i] τ_t is the fluorescence lifetime.

Table 2 Absorption and emission maxima of compounds in mixed solvents of toluene–acetonitrile ([dye] = 1×10^{-5} M)

	T1		**T2**		**T3**		**1**		**2**		**3**	
Solvent[a] (%)	λ^{a}_{max}/nm	λ^{fl}_{max}/nm	λ^{a}_{max}/nm	λ^{fl}_{max}/nm	λ^{a}_{max}/nm	λ^{fl}_{max}/nm	λ^{a}_{max}/nm	λ^{fl}_{max}/nm	λ^{a}_{max}/nm	λ^{fl}_{max}/nm	λ^{a}_{max}/nm	λ^{fl}_{max}/nm
0	440.0	493.6	439.0	495.0	440.0	493.6	458.0	513.4	473.0	501.0	476.5	506.0
20	442.0	546.8	439.5	546.8	440.0	543.8	462.0	550.6	479.5	549.0	482.0	552.0
40	440.5	557.2	439.5	555.4	437.5	556.6	463.0	565.0	479.5	564.2	481.5	564.2
60	440.5	562.6	438.5	561.8	437.0	562.8	462.5	569.6	479.5	568.8	482.0	576.0
80	438.5	570.8	437.5	569.4	437.5	569.4	460.5	577.6	478.0	577.0	480.5	576.8
100	437.5	573.8	436.5	570.4	436.0	573.8	458.5	581.8	476.0	578.8	478.0	583.2

[a] The numbers denote the volume percentage of acetonitrile in toluene.

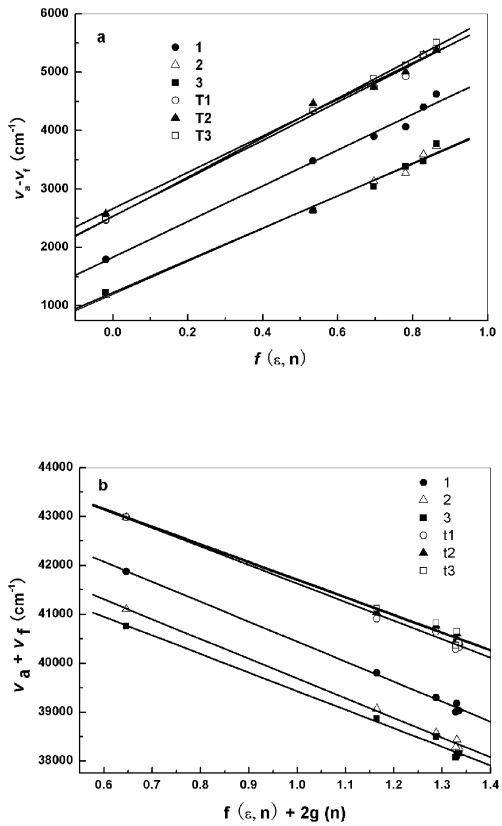

Fig. 3 Plot of $\tilde{\nu}_a - \tilde{\nu}_f$ (cm^{-1}) *vs.* $f(\varepsilon,n)$ (a) and $\tilde{\nu}_a + \tilde{\nu}_f$ (cm^{-1}) *vs.* $f(\varepsilon,n) + 2g(n)$ (b) of compounds in mixed solvents.

Table 3 Dipole moments, slope and correlation factor (r) of compounds

Molecule	Radius, a/Å	m_1/cm^{-1}	m_2/cm^{-1}	μ_g/D	μ_e/D	$\Delta\mu$/D
T1	5.55	3258.86	3795.60	0.60	7.93	7.32
T2	5.55	3117.53	3607.04	0.56	7.73	7.16
T3	5.55	3375.25	3611.97	0.26	7.72	7.45
1	6.27	3058.77	4086.93	1.43	9.95	8.52
2	6.81	2810.16	4038.56	2.02	11.26	9.24
3	7.84	2758.46	3800.04	2.14	13.45	11.31

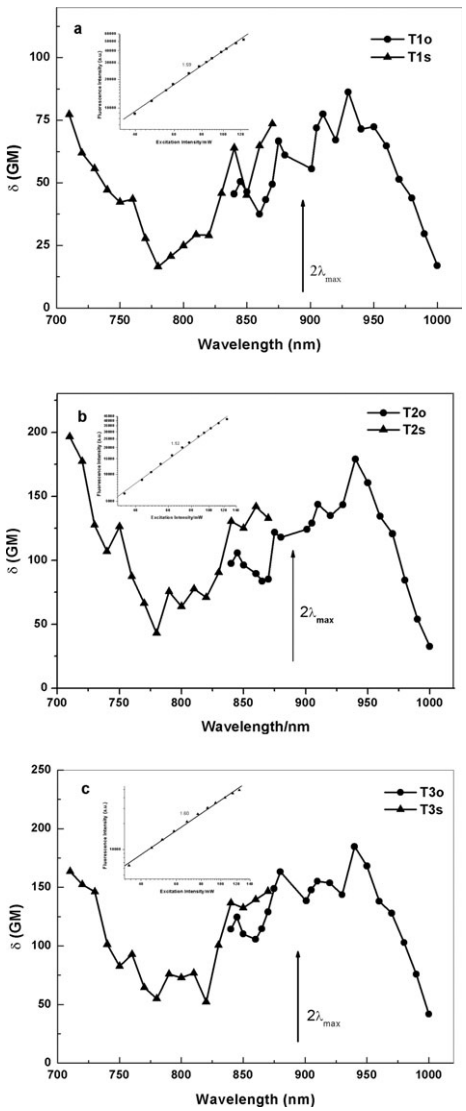

Fig. 4 Two-photon excitation spectra of **T1–T3** (2×10^{-4} M, in chloroform). The excitation sources are Tsunami (filled triangles) and OPA (filled circles), respectively. The inset shows logarithmic plots of TPA induced fluorescence *vs.* excitation power at 800 nm.

which lie in the range 780–850 nm are more likely corresponding to the S_0–S_2 transition (shown in Fig. 5(b) by taking **1** for example).

Normally, compounds with smaller excited state charge transfer ($\Delta\mu$) exhibit smaller TPA cross-sections,[8] so it is anticipated that the TPA capabilities of **T1–T3** will be smaller than those of **1–3**. However, it is still strongly unexpected that δ values of **T1–T3** are so small compared to those of **1–3** (shown in Table 1). This may be due to their different two-photon excited transitions patterns. Further, the factor $\Delta\mu_{s1-s2}$ should be considered for large δ values of **1–3**.[8] The ratio of δ_{max} of **T1–T3** is 1 : 2.08 : 2.33. Obviously,

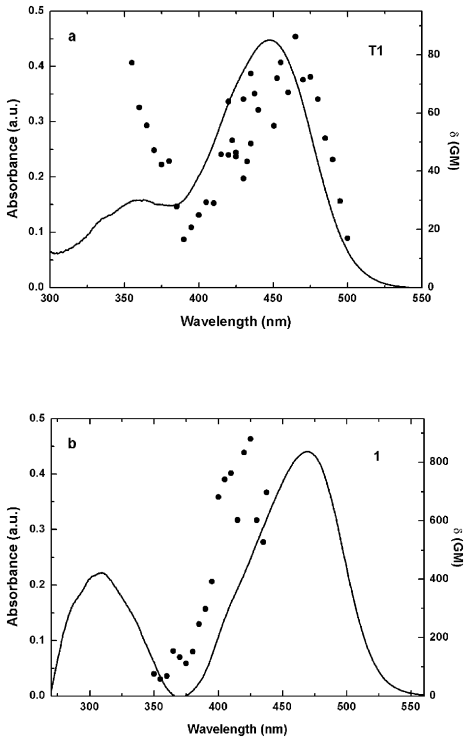

Fig. 5 Two-photon absorption spectra (filled circles) and linear absorption spectra of **T1** (a) and **1** (b).

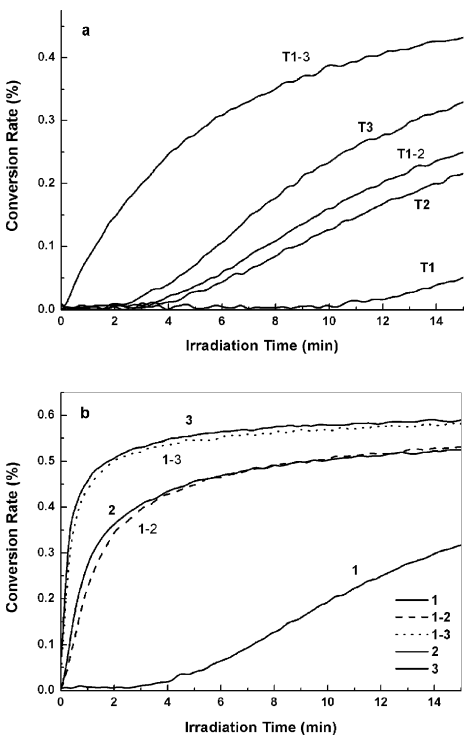

Fig. 6 Double-bond conversion rate *vs* irradiation time of (a) **T1–T3** and (b) **1–3**.

no cooperative enhancement effect exists in **T2** and **T3**. Contrarily, significant cooperative enhancements of δ are obtained in **2** and **3** compared to **1**. The results indicate clearly that the electronic coupling contribution is indispensable and is the major factor in the enhanced δ of multibranched molecules, and that the vibronic coupling contribution may be overrated in some discussions.[23]

3.4 Photosensitize efficiencies

The sensitizing efficiencies of these compounds to the commonly used co-initiator Omnicat 820 were investigated by one-photon photopolymerization. Through monitoring the relative change of the double bond absorption of acrylate monomers at 6164 cm^{-1} in the near-IR region, the sensitizing efficiencies of different compounds were determined and the results are shown in Fig. 6. It is clear that the sensitizing efficiencies of **T2**, **T3** are smaller than those of twice (**T1**–2) and three times (**T1**–3) the amount of **T1**. This may be due to the limited diffusion of chromophores with multibranched structures. On the other hand, it is interesting to notice that **2**, **3** exhibit equal initiating efficiencies compared to twice (**1**–2) and three times (**1**–3) that of **1**, respectively, though their absorption efficiency are correspondingly smaller at 473 nm. This indicates that the electronic coupling effect is beneficial not only to TPA cross-sections but also to photosensitizing efficiency of multibranched compounds.

Conclusions

A series of multibranched benzylidene cyclopentanone dyes (**T1–T3**) with non-conjugated central moiety were synthesized. Their one- and two-photon photophysical properties were systematically studied in comparison with corresponding triphenylamine derivatives (**1–3**). The results showed that without cross-conjugation, to increase the branch number simply increases the number density of chromophores, there being no electronic or vibronic coupling effect among branches in **T2** and **T3**. Contrarily, **2** and **3** exhibit larger fluorescent quantum yield, longer fluorescence lifetime, increased excited state charge transfer, and most importantly, cooperatively enhanced TPA cross-sections (δ) compared to monomer **1**. The electronic coupling is confirmed to be the main factor in the enhanced δ of multibranched compounds. Furthermore, it is indicated the electronic coupling effect is also beneficial to the photosensitizing efficiency of **2** and **3**.

Acknowledgements

This work was supported by NSFC (No. 50403030) and NSAF of China (No. 10776033), the Science and Technology Innovation Fund of CAS.

References

1 M. Göppert-Mayer, *Ann. Phys.*, 1931, **9**, 273.
2 W. Kaiser and C. G. B. Garrett, *Phys. Rev. Lett.*, 1961, **7**, 229.
3 W. Denk, J. H. Strickler and W. W. Webb, *Science*, 1990, **248**, 73.
4 D. A. Parthenopoulos and P. M. Rentzepis, *Science*, 1989, **245**, 843.
5 S. Maruo, O. Nakamura and S. Kawata, *Opt. Lett.*, 1997, **22**, 132.
6 J. E. Ehrlich, X. L. Wu, I.-Y. S. Lee, Z.-Y. Hu, H. Röckel, S. R. Marder and J. W. Perry, *Opt. Lett.*, 1997, **22**, 1843.
7 J. D. Bhawalkar, N. D. Kumar, C. F. Zhao and P. N. Prasad, *J. Clin. Laser Med. Surg.*, 1997, **15**, 201.
8 M. Albota, D. Beljonne, J.-L. Bredas, J. E. Ehrlich, J.-Y. Fu, A. A. Heikal, S. E. Hess, T. Kogej, M. D. Levin, S. R. Marder,

D. McCord-Maughon, J. W. Perry, H. Rockel, M. Rumi, G. Subramaniam, W. W. Webb, X.-L. Wu and C. Xu, *Science*, 1998, **281**, 1653.
9 B. A. Reinhardt, L. L. Brott, S. J. Clarson, A. G. Dillard, J. C. Bhatt, R. Kannan, L. Yuan, G. S. He and P. N. Prasad, *Chem. Mater*., 1998, **10**, 1863.
10 S.-J. Chung, K.-S. Kim, T.-C. Lin, G. S. He, J. Swiatkiewitz and P. N. Prasad, *J. Phys. Chem. B*, 1999, **103**, 10741.
11 O. Mongin, L. Porrès, L. Moreaux, J. Mertz and M. Blanchard-Desce, *Org. Lett*., 2002, **4**, 719.
12 K. D. Belfield, A. R. Morales, J. M. Hales, D. J. Hagan, E. W. Van Stryland, V. M. Chapela and J. Percino, *Chem. Mater*., 2004, **16**, 2267.
13 A. Adronov, J. M. J. Fréchet, G. S. He, K.-S. Kim, S.-J. Chung, J. Swiatkiewicz and P. N. Prasad, *Chem. Mater*., 2000, **12**, 2838.
14 B. R. Cho, K. H. Son, S. H. Lee, Y.-S. Song, Y.-K. Lee, S.-J. Jeon, J. H. Choi, H. Lee and M. Cho, *J. Am. Chem. Soc*., 2001, **123**, 10039.
15 J. Yoo, S. K. Yang, M.-Y. Jeong, H. C. Ahn, S.-J. Jeon and B. R. Cho, *Org. Lett*., 2003, **5**, 645.
16 M. Drobizhev, A. Karotki, Y. Dzenis, A. Rebane, Z.-Y. Suo and C. W. Spangler, *J. Phys. Chem. B*, 2003, **107**, 7540.
17 L. Porrès, O. Mongin, C. Katan, M. Charlot, T. Pons, J. Mertz and M. Blanchard-Desce, *Org. Lett*., 2004, **6**, 47.
18 B. J. Zhang and S. J. Jeon, *Chem. Phys. Lett*., 2003, **377**, 210.
19 O. Mongin, J. Brunel, L. Porrès and M. Blanchard-Desce, *Tetrahedron Lett*., 2003, **44**, 2813.
20 Q.-D. Zheng, G. S. He and P. N. Prasad, *Chem. Mater*., 2005, **17**, 6004.
21 F. Terenziani, C. L. Droumaguet, C. Katan, O. Mongin and M. Blanchard-Desce, *ChemPhysChem*, 2007, **8**, 723.
22 G. P. Bartholomew, M. Rumi, S. J. K. Pond, J. W. Perry, S. Tretiak and G. C. Bazan, *J. Am. Chem. Soc*., 2004, **126**, 11529.
23 P. Macak, Y. Luo, P. Norman and H. Ågren, *J. Chem. Phys*., 2000, **113**, 7055.
24 J. Wu, Y.-X. Zhao, X. Li, M.-Q. Shi, F.-P. Wu and X.-Y. Fang, *New J. Chem*., 2006, **30**, 1098.
25 Y.-X. Zhao, X. Li, F.-P. Wu and X.-Y. Fang, *J. Photochem. Photobiol., A: Chem*., 2006, **177**, 12.
26 (*a*) B. M. Monroe, W. K. Smothers, D. E. Keys, R. R. Krebs, D. J. Mickish, A. F. Harrington, S. R. Schicken, M. K. Armstrong, D. M. T. Chan and C. I. Weathers, *J. Imaging Sci*., 1991, **35**, 19; (*b*) B. M. Monroe, *US. Pat*., 4,987,230, 1991.
27 E.-J. Wang, J. Li and Y.-Y. Yang, *J. Photopolym. Sci. Technol*., 1991, **4**, 157.
28 T. Wang, F.-P. Wu and M.-Q. Shi, *Chem. Res. Chin. Univ*., 2003, **19**, 470.
29 F. E. E. Germann and O. S. Knight, *J. Am. Chem. Soc*., 1933, **55**, 4150.
30 J. P. Mason and D. J. Gasch, *J. Am. Chem. Soc*., 1938, **60**, 2816.
31 A. Nelson, J. M. Belitsky, S. Vidal, C. S. Joiner, L. G. Baum and J. F. Stoddart, *J. Am. Chem. Soc*., 2004, **126**, 11914.
32 E. Wilson and M. Tishler, *J. Am. Chem. Soc*., 1951, **73**, 3635.
33 L. Bilot and A. Kawski, *Z. Naturforsch., Teil A*, 1962, **17**, 621.
34 A. Kawski, in *Progress In Photochemistry and Photophysics*, ed. J. F. Rabek, CRC Press, Boca Raton, FL, 1992, vol. 5, pp. 1–47.
35 A. Kawski, *Z. Naturforsch., Teil A*, 2002, **57**, 255.
36 J. N. Demas and G. A. Crosby, *J. Phys. Chem*., 1971, **75**, 991.
37 C. Xu and W. W. Webb, *J. Opt. Soc. Am. B*, 1996, **13**, 481.

